Postintercalative Polymerization of Aniline and Its Derivatives in Layered Metal Phosphates

Yu-Ju Liu and Mercouri G. Kanatzidis*,†

Department of Chemistry, and Center for Fundamental Materials Research, Michigan State University East Lansing, Michigan 48824

Received February 14, 1995. Revised Manuscript Received May 11, 1995⊗

The formation of polyaniline in the layered metal phosphates, α-$Ti(HOPO_3)_2 \cdot H_2O$, α-$Zr(HOPO_3)_2 \cdot H_2O$, and $HUO_2PO_4 \cdot 4H_2O$ is reported. Aniline and *N*-phenyl-1,4-phenylenediamine (PPDA) are intercalated in the layered phosphates to form the precursors for polymerization. X-ray diffraction patterns show interlayer expansions with titanium phosphate and zirconium phosphate, consistent with a bilayer of these molecules in the gallery. In contrast, only a monolayer is intercalated in uranyl phosphate. After thermal treatment at 130 °C in air, the intercalated aniline and PPDA are slowly polymerized by ambient oxygen. The formation of polyaniline was confirmed by FT-IR, UV/vis and EPR spectroscopies as well as magnetic susceptibility measurements. Following polymerization, the interlayer spacing slightly increases from 10.46 to 11.8 Å for anilinium/uranyl phosphate but dramatically decreases from 28.3 to 20.5 Å for PPDA/$Zr(HOPO_3)_2$ and from 18.87 to 13.25 Å for anilinium/$Ti(HOPO_3)_2$, suggesting a monolayer of polyaniline inside the uranyl phosphate and titanium phosphate structures but a bilayer in $Zr(HOPO_3)_2$. Gel permeation chromatography was used to determine the MW of the intercalated polyaniline. Prolonged heating in air results in cross-linked polymer in the galleries. All compounds are insulators.

Introduction

In recent years, inclusion of conjugated polymers into inorganic host lattices has been the subject of considerable investigation.[1,2] The inorganic lattices provide confined spaces which can force the polymer molecules into organized arrays, thereby modifying their bulk properties. In such systems the polymer chains are reasonably isolated from one another by the inorganic material and may provide an opportunity to study spectroscopically the properties of single chains.[3] Polyaniline (PANI)[4] has been inserted into several inorganic hosts by different methods. One approach uses hosts with sufficient oxidative power to intercalate and polymerize aniline in situ. FeOCl[5] and V_2O_5 xerogel[6] are examples of such hosts. This type of compounds is comparatively rare, because most host materials are either nonoxidizing or weakly oxidizing. Therefore, to polymerize monomers inside host materials with insufficient oxidative power, external oxidants must be used. Inoue and co-workers reported an electrochemical polymerization of intercalated aniline in montmorillonite.[7] Bein et al. used $(NH_4)_2S_2O_8$ to successfully polymerize the intercalated aniline in zeolites.[8] The same method was also applied to MoO_3.[9] Another method to insert conjugated polymers in host materials is to directly modify the oxidative power of the host by incorporation of oxidants. By preintercalating Cu^{2+} in a host, an in situ polymerization of aniline can be accomplished, as in the case of silicates[10] and in zirconium phosphate.[11] Recently, we reported direct inclusion of polyaniline into MoS_2 by taking advantage of the exfoliation property of this dichalcogenide.[12]

Layered metal phosphates are known to possess rich intercalation chemistry.[13] The protons in the layers can

† Camille and Henry Dreyfus Teacher Scholar 1993–95.

⊗ Abstract published in *Advance ACS Abstracts,* June 15, 1995.

(1) (a) Kanatzidis, M. G.; Tonge, L. M.; Marks, T. J.; Marcy, H. O.; Kannewurf, C. R. *J. Am. Chem. Soc.* **1987**, *109*, 3797–3799. (b) Wu, C.-G.; Kanatzidis, M. G.; Marcy, H. O.; DeGroot, D. C.; Kannewurf, C. R. *Polym. Mater. Sci. Eng.* **1989**, *61*, 969–973. (c) Kanatzidis, M. G.; Wu, C.-G.; Marcy, H. O.; DeGroot, D. C.; Kannewurf, C. R. *Chem. Mater.* **1990**, *2(3)*, 222–224. (d) Wu, C.-G.; Marcy, H. O.; DeGroot, D. C.; Schindler, J. L.; Kannewurf, C. R.; Leung, W.-Y.; Benz, M.; LeGoff, E.; Kanatzidis, M. G. *Synth. Met.* **1991**, *41–43*, 797–803. (e) Wu, C.-G.; Marcy, H. O.; DeGroot, D. C.; Schindler, J. L.; Kannewurf, C. R.; Kanatzidis, M. G. *Synth. Met.* **1991**, *41–43*, 693–698.

(2) (a) Day, P.; Ledsham, R. D. *Mol. Cryst. Liq. Cryst.* **1982**, *86*, 163–174. (b) Tieke, B. *Mol. Cryst. Liq. Cryst.* **1983**, *93*, 119–145. (c) Pillion, J. E.; Thompson, M. E. *Chem. Mater.* **1991**, *3*, 777–779. (d) Enzel, P.; Bein, T. *Chem. Mater.* **1992**, *4*, 819–824. (e) (a) Nazar, L. F., Zhang, Z; Zinweg, D *J. Am. Chem. Soc.* **1992**, *114*, 6239–6240

(3) Caspar, J. V.; Ramamurthy, V.; Corbin, D. R. *J. Am. Chem. Soc.* **1991**, *113*, 600–610.

(4) (a) *Handbook of Conducting Polymers*; Skotheim, T. A., Ed.; Marcel Dekker: New York, 1986; Vol. 1, and 2. (b) Huang, W.-S.; Humphrey, B. D.; MacDiarmid, A. G. *J. Chem. Soc., Faraday Trans* **1986**, *82*, 2385–2400. (c) Kanatzidis, M. G. *Chem. Eng. News* **1990**, *68 (49)*, 36–50. (d) Geniès, E. M.; Boyle, A.; Lapkowski, M.; Tsintavis, C. *Synth. Met.* **1990**, *36*, 139–182.

(5) (a) Kanatzidis, M. G.; Wu, C.-G. ; Marcy, H. O.; Kannewurf, C. R. *Adv. Mater.* **1990**, *2*, 364–366. (b) Wu, C.-G. ; DeGroot, D. C.; Marcy, H. O.; Schindler, J. L.; Kannewurf, C. R.; Bakas, T.; Papaefthymiou, V.; Hirpo, W.; Yesinowski, J. P.; Liu, Y.-J.; Kanatzidis, M. G. *J. Am. Chem. Soc.*, in press.

(6) Kanatzidis, M. G.; Wu, C.-G.; Marcy, H. O.; Kannewurf, C. R. *J. Am. Chem. Soc.* **1989**, *111*, 4139–4141.

(7) Inoue H.; Yoneyama, H. *J. Electroanal. Chem.* **1987**, *233*, 291–295.

(8) Enzel P.; Bein, T *J. Phys. Chem.* **1989**, *93*, 6270–6272.

(9) (a) Bissessur, R.; DeGroot, D. C.; Schindler, J. L.; Kannewurf, C. R.; Kanatzidis, M. G. *J. Chem. Soc., Chem. Commun.* **1993**, 687–689.

(10) Mehrotra, V.; Giannelis, E. P. *Mater. Res. Soc. Symp. Proc.* **1990**, *171*, 39–44.

(11) Bonnet, B.; Meijad, R. E.; Herzog, M.-H.; Jones, D. J.; Roziére, J. *Mater. Sci. Forum*, **1992**, *91–92*, 177–182.

(12) Kanatzidis, M. G.; Bissessur, R.; DeGroot, D. C.; Schindler, J. L.; Kannewurf, C. R. *Chem. Mater.* **1993**, *5 (5)*, 595–596.

(13) (a) Clearfield, A. *Comments Inorg. Chem.* **1990**, *10 (2&3)*, 89–128. (b) Clearfield, A. *Chem. Rev.* **1988**, *88*, 125–148. (c) Alberti, G. *Acc. Chem. Res.* **1978**, *11*, 163–170. (d) Cao, G.; Rabenberg, L. K.; Nunn, C. M.; Mallouk, T. E. *Chem. Mater.* **1991**, *3*, 149–156. (e) Johnson, J. W.; Jacobson, A. J.; Butler, W. M.; Rosenthal, S. E.; Brody, J. F.; Lewandowski, J. T. *J. Am. Chem. Soc.* **1989**, *111*, 381–383.

0897-4756/95/2807-1525$09.00/0

be exchanged with cations or neutralized with bases. The resulting intercalation compounds, depending on the guest molecules, can have diverse properties.[13,14] Here we have intercalated aniline and its dimer *N*-phenyl-1,4-phenylenediamine (PPDA) in layered metal phosphates, and used oxygen to polymerize them topotactically to polyaniline. In this method, the polymerization is carried out by simple thermal treatment of the amine intercalated compounds in air. The thought to use oxygen for polymerization derives from a recent publication where we reported that anilinium molecules, intercalated in $V_2O_5{\cdot}nH_2O$, undergo intralamellar conversion to PANI upon exposure to ambient oxygen.[15] The polymerization, which proceedes at room temperature in this case, seems to be catalyzed by V^{5+} ions in the inorganic lattice. Traditional oxidants, such as $(NH_4)_2S_2O_8$, $FeCl_3$, lead to ion-exchange reactions which compete with the intralayer polymerization reaction and cause polyaniline to form outside the host crystallites. The ion-exchange reaction is totally avoided when oxygen is used as the oxidant. We have already reported preliminary results from this work in the case of uranyl phosphate.[16] Herein, we report the details of this type of reaction and its application to α-titanium phosphate and α-zirconium phosphate.

Experimental Section

Materials. Zirconyl chloride octahydrate ($ZrOCl_2{\cdot}8H_2O$), titanium tetrachloride ($TiCl_4$), aniline, and *N*-phenyl-1,4-phenylenediamine (PPDA) were used as received from Aldrich Chemical Co., Milwaukee, WI. Uranyl nitrate hexahydrate ($UO_2(NO_3)_2{\cdot}6H_2O$) was obtained from J. T. Baker Chemical Co., Phillipsburg, NJ. Phosphoric acid (85%) and hydrofluoric acid (50%) were purchased from Fisher Scientific Co., Fairlawn, NJ. Catechol was received from Mallinckrodt Inc., Paris, KY. Elemental analyses were done by Galbraith Laboratories, Knoxville, TN, and Oneida Research Services, Inc., Whitesboro, NY.

Measurements. Optical diffuse reflectance measurements were made at room temperature with a Shimadzu UV-3101PC double beam, double-monochromator spectrophotometer operating in the 200–2500 nm region. The instrument was equipped with an integrating sphere and controlled by a personal computer. The digitized spectra were processed using the Kaleidagraph software program. $BaSO_4$ powder was used as reference (100% reflectance). The data were processed as described earlier.[17] Infrared spectra were collected from 4000 to 400 cm^{-1} with a resolution of 4 cm^{-1} on a Nicolet 740 FT-IR spectrometer. Samples were recorded in pressed KBr matrices under N_2 flow.

Thermogravimetric analysis (TGA) was performed on a Shimadzu TGA-50. Typically 5–10 mg of sample was heated in a quartz crucible from room temperature to 1000 °C with a heating rate of 5 °C/min in air or nitrogen. For differential scanning calorimetry (DSC) we used a Shimadzu DSC-50 thermal analyzer. Samples (3–5 mg) were put in a aluminum pan and heated to 200 °C with 5 °C/min. An empty aluminum pan was taken as the reference.

Variable temperature magnetic susceptibility data were collected from 5 to 300 K on a S.H.E. Corp. SQUID system at a magnetic field of 400 G. The data were corrected for diamagnetic components with values obtained from the literature.[18]

Scanning electron microscopy (SEM) was done on a JEOL-JSM 35 CF with an accelerating voltage of 15 kV. Samples were glued to the microscope sample holder with conducting graphite paint.

Molecular weights were determined with a Shimadzu LC-10A HPLC system with a PLgel 5 μm mix column. The measurements were done at 75 °C with *N*-methylpyrrolidone, NMP (containing 0.5 wt % LiCl), as the eluent. The elution rate was 0.2 mL/min. Polystyrene of known molecular weights was used as a MW standard. The detector was a UV/vis lamp which was set at 270 nm for polystyrene and 315 nm for polyaniline. Roughly, an amount of 0.1 mg of polyaniline was dissolved in 5 mL of NMP. The resulting purplish blue solution was prefiltered with a 4.5 μm of frit and then injected into the column with a volume of 10 μL.

X-ray diffraction was carried out on a Rigaku rotating anode X-ray powder diffractometer, Rigaku-Denki/RW400F2 (Rotaflex), at 45 kV and 100 mA with a scintillation counter detector and a graphite monochromator to yield Cu Kα (wavelength 1.541 84 Å) radiation. Data were collected at room temperature over the range $2° \le 2\theta \le 60°$ in increments of 0.01°. The X-ray coherence length of the crystallites was calculated according to the Scherrer formula[19] $L_{hkl} = K\lambda/B \cos\theta$. L is the coherence length along directions perpendicular to the Miller index planes (hkl), λ is the wavelength of the X-rays used, K is Scherrer's constant and has a value of 0.9, θ is the Bragg angle, and B is the peak width at half-height in radians. Instrumental broadening was accounted for by using values obtained from the reflections of a polycrystalline FeOCl sample.

Electron paramagnetic resonance (EPR) spectroscopy was obtained using a Varian E-4 spectrometer operating at 9.5 GHz (X band) and at room temperature. Solid samples were scanned from 2700 to 3700 G at 8 G field modulation and 0.03 s time constant. The g value was obtained with reference to the standard diphenylpicrylhydrazine (DPPH).

Preparation of Layered Metal Phosphates. $HUO_2PO_4{\cdot}4H_2O$ (HUP), α-$Zr(HOPO_3)_2{\cdot}H_2O$ (α-ZrP), and α-$Ti(HOPO_3)_2{\cdot}H_2O$ (α-TiP) were prepared according to reported methods.[20] The compound HUP is a luminous yellow solid which precipitates from H_3PO_4 and $UO_2(NO_3)_2$ in aqueous solution.[21] α-ZrP is a white crystalline powder prepared by adding concentrated H_3PO_4 to $ZrOCl_2$ solution in the presence of HF. Crystalline α-TiP was synthesized by refluxing its gel in concentrated H_3PO_4. The gel was prepared by slowly adding $TiCl_4$ into H_3PO_4 solution.

Preparation of $(C_6H_5NH_3)_{1.0}UO_2PO_4{\cdot}0.4H_2O$ (AUP) and $H_{0.12}(C_6H_5NHC_6H_4NH_3)_{0.88}UO_2PO_4$ (A_2UP). Excess aniline or PPDA was added into a flask containing 1.0 g of $HUO_2PO_4{\cdot}4H_2O$ and 80 mL of distilled water. The mixture was stirred for 1 day at room temperature. The product was filtered and then washed with acetone. After drying overnight under N_2, AUP is pale yellow and A_2UP is pale gray. Anal. Calcd for $(C_6H_5NH_3)_{1.0}UO_2PO_4{\cdot}0.4H_2O$: C, 15.40%; H, 1.89%; N, 3.0%. Found: C 15.48%, H 1.78%; N 2.95%. The composition of A_2UP, calculated from thermogravimetric analysis (TGA), is $H_{0.12}(C_6H_5NHC_6H_4NH_3)_{0.88}UO_2PO_4$.

Preparation of $H_{0.6}(C_6H_5NH_3)_{1.4}Ti(PO_4)_2$ (ATiP). An amount of 1.0 g (3.88 mmol) of $Ti(HOPO_3)_2{\cdot}H_2O$ and 1.44 g (15.48 mmol) of aniline were introduced into a 23 mL auto-

(14) (a) Olken, M. M.; Biagioni, R. N.; Ellis, A. B. *Inorg. Chem.* **1983**, *22*, 4128–4134. (b) Hunsberger, L. R.; Ellis, A. B. *Coord. Chem. Rev.* **1990**, *97*, 209–224.

(15) Liu, Y.-J.; DeGroot, D. C.; Schindler, J. L.; Kannewurf, C. R.; Kanatzidis, M. G. *J. Chem. Soc. Chem. Commun.* **1993**, 593–596.

(16) Liu, Y.-J.; Kanatzidis, M. G. *Inorg. Chem.* **1993**, *32 (14)*, 2989–2991.

(17) McCarthy, T. J.; Ngeyi, S.-P.; Liao, J.-H.; DeGroot, D.; Hogan, T.; Kannewurf, C. R.; Kanatzidis, M. G. *Chem. Mater.* **1993**, *5*, 331–340.

(18) *Theory and Applications of Molecular Paramagnetism*; Boudreaux, E. A., Mulay, L. N., Eds.; John Wiley &Sons: New York, 1976.

(19) Klug, H. P.; Alexander, L. E. *X-ray Diffraction Procedures for Polycrystalline and amorphous Materials*; John Wiley & Sons: New York, 1962; pp 491–538.

(20) (a) Weigel, F.; Hoffmann, G. *J. Inorg. Nucl. Chem.* **1976**, *44*, 99–123. (b) Alberti, G.; Torracca, E. *J. Inorg. Nucl. Chem.* **1968**, *30*, 317–318. (c) Alberti, G.; Cardini-Galli, P.; Costantino, U.; Torracca, E. *J. Inorg. Nucl. Chem.* **1967**, *29*, 571–578.

(21) (a) Morosin, B. *Phys. Lett.* **1978**, *65A*, 53 (b) Shilton, M. G.; Howe, A. T. *J. Solid State Chem.* **1980**, *34*, 137. (c) Lloyd, M. H.; Bischoff, K.; Peng, K.; Nissen, H. U.; Wessicken, R. *J. Inorg. Nucl. Chem.* **1976**, *38*, 1141.

clave. The autoclave was put into a furnace with a constant temperature of 130 °C for 3 days. After cooling to room temperature, the white product was filtered and washed with acetone. The composition of ATiP, calculated from TGA, is $H_{0.6}(C_6H_5NH_3)_{1.4}Ti(PO_4)_2$.

Preparation of $H_{0.7}(C_6H_5NH_3)_{1.3}Zr(PO_4)_2$ (AZrP) and $H_{0.6}(C_6H_5NHC_6H_4NH_3)_{1.4}Zr(PO_4)_2$ (A_2ZrP). Excess PPDA, or aniline, was added to α-$Zr(HOPO_3)_2{\cdot}H_2O$ (0.5 g) in 50 mL of distilled water and the mixture was stirred for 2 days. The reaction temperature was ~25 °C for aniline and 80 °C for PPDA. The products were removed by filtration, washed with acetone, and then dried under N_2. AZrP is white and A_2ZrP is pale gray. Anal. Calcd for $H_{0.6}(C_6H_5NHC_6H_4NH_3)_{1.4}Zr(PO_4)_2$: C 37.3%, H 3.5%, N 7.26%. Found: C 37.6%; H 3.54%, N 7.03%. The composition of AZrP, calculated from TGA, is $H_{0.7}(C_6H_5NH_3)_{1.3}Zr(PO_4)_2{\cdot}0.1H_2O$.

Preparation of $(PANI)_{0.94}UO_2PO_4{\cdot}0.5H_2O$ (PUP), $(PANI)_{0.8}Ti(PO_4)_2$ (PTiP), and $(PANI)_{2.4}Zr(PO_4)_2$ (PZrP) from AUP, ATiP, and A_2ZrP. Quantities of AUP, A_2ZrP, and ATiP were introduced into small open Pyrex containers which were put into a furnace with a constant temperature of 130 ± 3 °C. After several weeks, black products were obtained. Anal. Calcd for $(PANI)_{0.94}UO_2PO_4{\cdot}0.5H_2O$: C 14.7%, H 2.86%, N 1.24%. Found: C 14.1%, N 1.27%, H 2.83%. Anal. Calcd for $(PANI)_{2.4}Zr(PO_4)_2$: C, 36.67%; H, 2.7%, N, 7.1%. Found: C 38.78%, N 6.52%, H 2.69%. The composition of PTiP, calculated from TGA, is $(PANI)_{0.8}Ti(PO_4)_2$. PANI in this case is taken as $-C_6H_4NH-$.

Extraction of Polyaniline from PUP. The compound PUP (0.1 g) was added to excess 20% HCl solution. After 1 day of stirring at room temperature, the black precipitate was collected by filtration, washed with water and acetone, and dried in air.

Extraction of Polyaniline from PTiP. The compound PTiP (0.1 g) was added to 50 mL of 20% HCl solution containing 1.5 g of catechol. The mixture was refluxed for 2 days and then cooled to room temperature. After filtration, the black residue was washed with water and acetone and dried in air.

Extraction of Polyaniline from PZrP. An amount of 0.20 g of PZrP was added to excess 10% HF solution. After ~12 h of stirring, the black precipitate was filtered, washed with water then with acetone, and dried in air. The base form of polyaniline was prepared by treating the extracted material with excess 0.1 M NH_4OH for ~12 h. The product was filtered, washed copiously with distilled water and acetone, and dried in air.

Results and Discussion

The objective of this study was the detailed characterization of the postintercalative redox polymerization of aniline and PPDA in several metal phosphate hosts. We begin with a discussion of the synthesis and product characterization, followed by spectroscopic, magnetic and molecular weight studies of the polymer products. The PPDA, which is an oxidatively coupled dimer of aniline, was used to probe the effect of monomer length on the reaction rate. The latter is not easily assessed a priori, because both an acceleration and deceleration relative to aniline depending on what mechanism is operable. For example, thermodynamically, a faster polymerization is expected for PPDA because the dimer is more easily oxidized. However, this bulky molecule, or its coupled oligomers, would be more sluggish and could get kinetically trapped in the host galleries giving rise to low molecular weight polymers or incomplete polymerization.

The reaction of layered metal phosphates with aniline and its derivatives results in intercalation compounds with well defined sharp X-ray powder diffraction patterns. For example, typical patterns for $H_{0.7}(C_6H_5NH_3)_{1.3}Zr(PO_4)_2$ (AZrP) and $H_{0.6}(C_6H_5NHC_6H_4NH_3)_{1.4}Zr(PO_4)_2$ (A_2ZrP) are given in Figure 1. Several strong (00l) peaks are observed, associated with scattering from the metal−phosphate layers, indicating high stacking order. The calculated interlayer distances are 19 Å for AZrP and 28.3 Å for A_2ZrP. Subtracting the inorganic layer thickness of ~6.6 Å, AZrP and A_2ZrP show net expansions of 12.4 and 21.7 Å, respectively, which are consistent with a bilayer of aniline and PPDA molecules in the interlayer regions. It is likely that the molecules are slightly tilted with respect to the layers. $H_{0.6}(C_6H_5NH_3)_{1.4}Ti(PO_4)_2$ (ATiP) probably also has a bilayer of anilinium molecules in the interlayer space. However, no intercalation was observed between PPDA and TiP. In contrast to the group IV phosphates above, $(C_6H_5NH_3)_{1.0}UO_2PO_4{\cdot}0.4H_2O$ (AUP) and $H_{0.12}(C_6H_5NH\text{-}C_6H_4NH_3)_{0.88}UO_2PO_4$ (A_2UP) show much smaller net expansions, suggesting the presence of a monolayer of organic guests. The interlayer distances and compositions of all compounds reported here are summarized in Table 1.

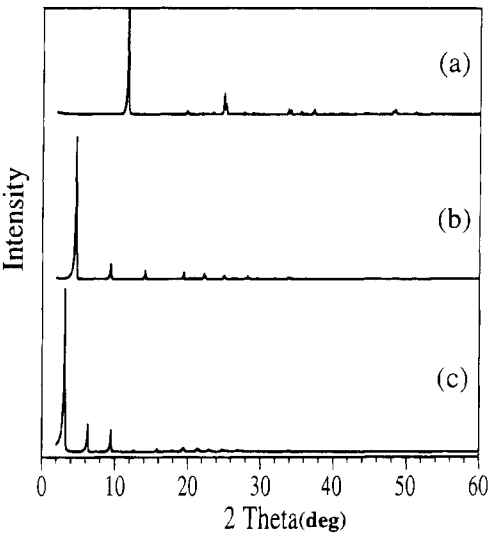

Figure 1. Powder X-ray diffraction patterns of (a) α-$Zr(HOPO_3)_2{\cdot}H_2O$, (b) $H_{0.7}(C_6H_5NH_3)_{1.3}Zr(PO_4)_2$, and (c) $H_{0.6}(C_6H_5NHC_6H_4NH_3)_{1.4}Zr(PO_4)_2$.

Thermal treatment of the intercalates at 130 °C in air results in a gradual color change from yellow or pale gray to dark green and finally to black. The process takes 4 days for AUP, 8 days for ATiP, and only 1 day for A_2ZrP and A_2UP. The color change is, indeed, associated with the polymerization of aniline and PPDA. This is confirmed by FT-IR spectroscopy, which shows that the vibration bands of the monomers and dimers gradually decrease in intensity while the vibration bands of PANI quickly dominate the spectra. The FT-IR spectral changes in the case of AUP are shown in Figure 2. Before thermal treatment, AUP shows the characteristic vibrations of anilinium at ~3000, 2600, and 1500 cm^{-1}, consistent with an acid−base intercalation reaction, where the protons transfer from the layers to aniline. However, the broad vibration bands at 3490 and 3380 cm^{-1}, and a doublet at ~750 and ~690 cm^{-1} in the spectrum also imply the presence of neutral aniline molecules in the interlayer galleries. After 1 week, the absorption bands at ~3400−~2800 cm^{-1} (originating from the C−H, NH_3^+, and NH_2 groups) weaken and eventually are masked completely by an emerging strong electronic transition from PANI, which

Table 1. Summary of Compositions and Interlayer Spacings of Aniline and PPDA[a] Intercalated Metal Phosphates

inorganic host	organic guest	product composition	interlayer spacing (Å)	net expansion (Å)
HUP		$HUO_2PO_4{\cdot}4H_2O$	8.69	~2.3
HUP	aniline	$(C_6H_5NH_3)_{1.0}UO_2PO_4{\cdot}0.4H_2O$	10.46	~4.1
HUP	PPDA	$H_{0.12}(C_6H_5NHC_6H_4NH_3)_{0.88}UO_2PO_4$	18.39	~12.0
ZrP		$Zr(HOPO_3)_2{\cdot}H_2O$	7.60	~1.0
ZrP	aniline	$H_{0.7}(C_6H_5NH_3)_{1.3}Zr(PO_4)_2$	19.00	~12.4
ZrP	PPDA	$H_{0.6}(C_6H_5NHC_6H_4NH_3)_{1.4}Zr(PO_4)_2$	28.30	~21.7
TiP		$Ti(HOPO_3)_2{\cdot}H_2O$	7.57	~1.0
TiP	aniline	$H_{0.6}(C_6H_5NH_3)_{1.4}Ti(PO_4)_2$	18.87	~12.3

[a] PPDA = *N*-phenyl-1,4-phenylenediamine.

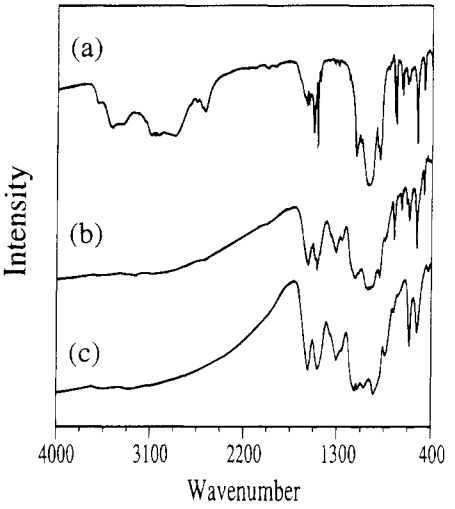

Figure 2. FT-IR spectra of $(C_6H_5NH_3)_{1.0}UO_2PO_4{\cdot}0.4H_2O$ (AUP) under thermal treatment for (a) 0 week, (b) 1 week, and (c) 3 weeks.

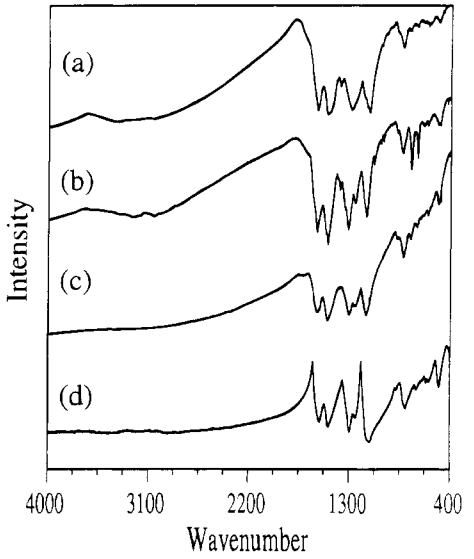

Figure 3. FT-IR of extracted PANI from (a) PUP, (b) PZrP, (c) PTiP, and (d) bulk PANI.

starts from ~1800 cm^{-1} and extends to the visible region. At the same time, the IR spectrum of PANI is clearly observed while the vibration bands of anilinium disappear within 3 weeks. Under the same conditions, complete polymerization takes place within ~4 weeks for ATiP but is even slower for A_2ZrP and A_2UP. The FT-IR spectra of the last two compounds still show significant amount of PPDA. The FT-IR spectra of the polymers extracted from the framework are shown in Figure 3, where the characteristic vibrations of bulk PANI (emeraldine form) are clearly observed in all cases, confirming that they are PANI. Their frequencies and corresponding vibration modes are listed in Table 2. Compared with bulk PANI, the frequency and shape of the extracted PANI are respectively slightly higher and sharper. This is either due to the shorter polymer chain length (see below) or to the formation of cross-linked PANI, which has been reported to form when PANI is heated.[22] Although color changes were also observed in AZrP, the FT-IR spectrum of the extracted organic species, surprisingly, is not PANI. The band at ~1300 cm^{-1} which is characteristic of PANI is weak and the bands at ~1100 and ~800 cm^{-1} are nearly absent, indicating that the number of C–H bending vibrations is reduced, consistent with a significantly cross-linked material.

Attempts to polymerize the intercalated monomers with other oxidants such as $(NH_4)_2S_2O_8$ and $FeCl_3$ did not yield intercalated PANI, instead, ion-exchange was observed followed by polymerization on the particle surfaces. In the absence of oxygen the precursor compounds show no color or other spectroscopic changes confirming that oxygen is a necessary reagent for polymerization. This can be seen by TGA experiments under an oxygen and nitrogen atmosphere, as shown in Figure 4. That oxygen is key to the intralamellar polymerization is a significant finding in this work.

The precursor compounds show better thermal stability under oxygen than under nitrogen because of polymer formation during the experiment. For A_2ZrP, the weight loss begins at 250 °C under nitrogen but mainly at 400 °C under oxygen. For ATiP, the weight-loss begins at ~200 °C under nitrogen flow. However, under oxygen flow, two decomposition steps were observed at ~200 and ~400 °C. The weight loss starting at 200 °C is attributed to evolution of aniline as shown by mass spectrometry. The loss of aniline slows down the intralamellar polymerization and results in incomplete polymerization. In addition, DSC of A_2ZrP shows a slight endotherm to 200 °C under N_2 atmosphere, consistent with the loss of PPDA. However, an exotherm was observed at ~180 °C under oxygen, probably due to oxidation of PPDA.

SEM micrographs of the layered metal phosphates before and after intercalation show a similar platelike morphology, consistent with their layered structure. In general, the average particle size of uranyl phosphate

(22) (a) Rodrigue, D.; Snauwaert, P.; Demaret, X.; Riga, J.; Verbist, J. J. *Synth. Met.* **1991**, *41–43*, 769–773. (b) Scherr, E. M.; MacDiarmid, A. G.; Manohar, S. K.; Masters, J. G.; Sun, Y.; Tang, X.; Druy, M. A.; Glatkowski, P. J.; Cajipe, V. B.; Fischer, J. E.; Cromack, K. R.; Jozefowicz, M. E.; Ginder, J. M.; McCall, R. P.; Epstein, A. J. *Synth. Met.* **1991**, *41–43*, 735–738. (c) Epstein, A. J.; MacDiarmid, A. G. in *Lower-Dimensional Systems and Molecular Electronics*, Metzger, R. M.; Day, P.; Papavassiliou, G. C. Eds.; Plenum Press, New York, 1990.

Table 2. Infrared Vibration Energies of Extracted Polymer from Layered Metal Phosphates

	C–C ring stretching	C–H bending or C–N stretching	C–H bending (in-plane)	C–H bending (out-of-plane)
bulk PANI	1560, 1481	1292, 1249	1109	797
PANI from PUP[a]	1576, 1492	1280	1118	815
PANI from PTiP	1582, 1492	1301, 1250	1149	817
PANI from PZrP[b]	1594, 1492	1315, 1250	1155	830

[a] Polymerized from AUP. [b] Polymerized from A_2ZrP.

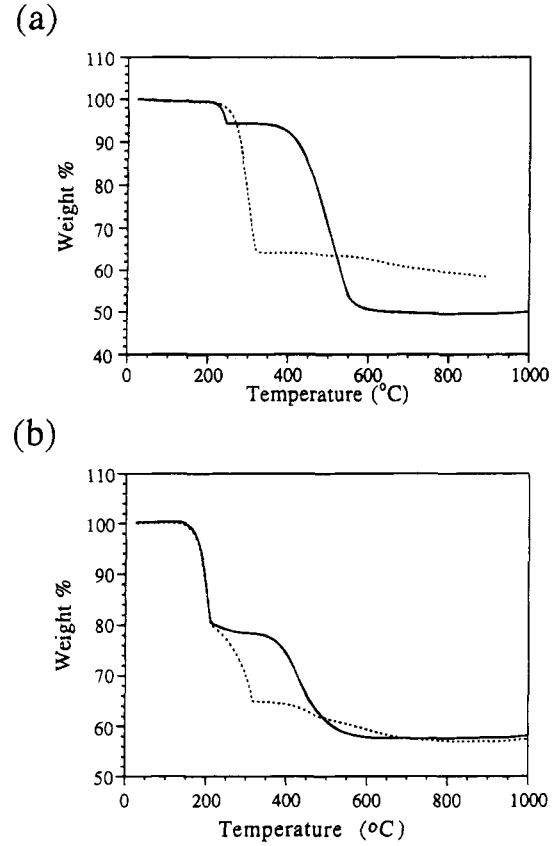

Figure 4. Thermogravimetric analysis diagrams of (a) A_2ZrP and (b) A_2TiP under air (—) and nitrogen flow (- - -).

is slightly larger than those of zirconium phosphate and titanium phosphate. The particles of the latter are in the submicrometer range regime. After intercalation, the platelike morphology and average particle size are maintained but microcracks develop on the surface of the crystallites. As the photographs of Figure 5 show, polymerization does not change the shape and size of the particles. The SEM micrographs confirm the crystalline nature of the inclusion compounds and are consistent with a topotactic polymerization inside the layers.

Solid-State UV/Vis/Near-IR Spectroscopy. Bulk polyaniline doped with camphor sulfonic acid (PANI·CMSA) is soluble in common solvents such as chloroform, *m*-cresol, pyrrolidine, and tripropylamine.[23] The as-made PANI·CMSA has a room-temperature conductivity similar to PANI (emeraldine salt) of ca. 2–5 S/cm.[24] However, recently MacDiarmid et al. showed that freestanding films of PANI·CMSA deposited from m-cresol solutions exhibit significantly higher conductivity of ca. 200 S/cm.[24] This increase in conductivity is attributed solely to a conformational change of the polymer chains from "coillike", in as-made form, to "rodlike" structure when processed from *m*-cresol. The properties of this processed polymer are completely different from its original form. First, it is significantly more ordered according to X-ray diffraction studies (e.g., the as-made bulk polymer itself is amorphous). Second, because of the increased metallic character of the *m*-cresol-processed polymer, its solid-state electronic spectrum exhibits dramatic differences from that of the bulk polymer. Thus, while the latter shows the usual localized polaron absorptions at 439 and 780 nm, films cast from *m*-cresol show the same absorption at 439 nm but, in addition, a very intense free-carrier tail absorption commencing at 1000 nm and increasing steadily in intensity to 2000 nm. The free-carrier tail is consistent with delocalized electrons in the polaron band along the now rodlike polymer backbone. The conductivity of the cast film dropped to the value of ca. 80 S/cm (still a very high value) upon removal of all the *m*-cresol and the free-carrier tail is still observable from solid-state UV–vis/near-IR spectroscopy. On the basis of these results, we believe we can use this type of spectroscopy as a diagnostic tool to probe the conformation of the PANI chains inside the inorganic hosts. Namely, since a coil conformation is not possible, based on the interlayer distances observed, inside the hosts discussed in this paper, the solid-state UV–vis/near-IR spectra of the polymer-containing intercalates should be quite similar to the spectrum of the rodlike PANI processed from *m*-cresol. In fact, electronic solid-state spectroscopy could serve as an additional tool to probe the location (i.e., inside vs outside the host) and the structure of the intercalated polymers. The technique would be particularly useful when no spectroscopic interference is presented by the host structure, as is the case here.

Indeed, solid state electronic spectra of PUP, PZrP, and PTiP show a high intensity absorption, beginning at ~450 nm and increasing in intensity at lower energies with a maximum at ~1500 nm, see Figure 6. This feature is similar to the free carrier tail observed for the PANI·CMSA/*m*-cresol system and can be attributed to delocalized electrons in the polaron band. Therefore, these data further support our conclusions that the polymer chains are indeed intercalated in these metal–phosphate hosts and suggest that the polymer chains are organized in the gallery parallel to one another as would be expected of straight chain molecules. Solid-state electronic spectroscopy provides an important complementary probe for the structure of conductive polymers, and particularly PANI, in constrained environments.

Structural Considerations. The polymerization process changes the orientation of the intercalated molecules as revealed from the interlayer distance of the host. After polymerization, the interlayer spacing slightly increased to 11.8 Å for PUP. Therefore, the

(23) Cao, Y.; Smith, P.; Heeger, A. J. *Synth. Met.* **1992**, *48*, 91–97.
(24) Min, Y.; MacDiarmid, A. G.; Epstein, A. *Polymer Prepr. (Am. Chem. Soc., Div. Polym. Chem.)* **1994**, *35*, No. 1, 231–232.

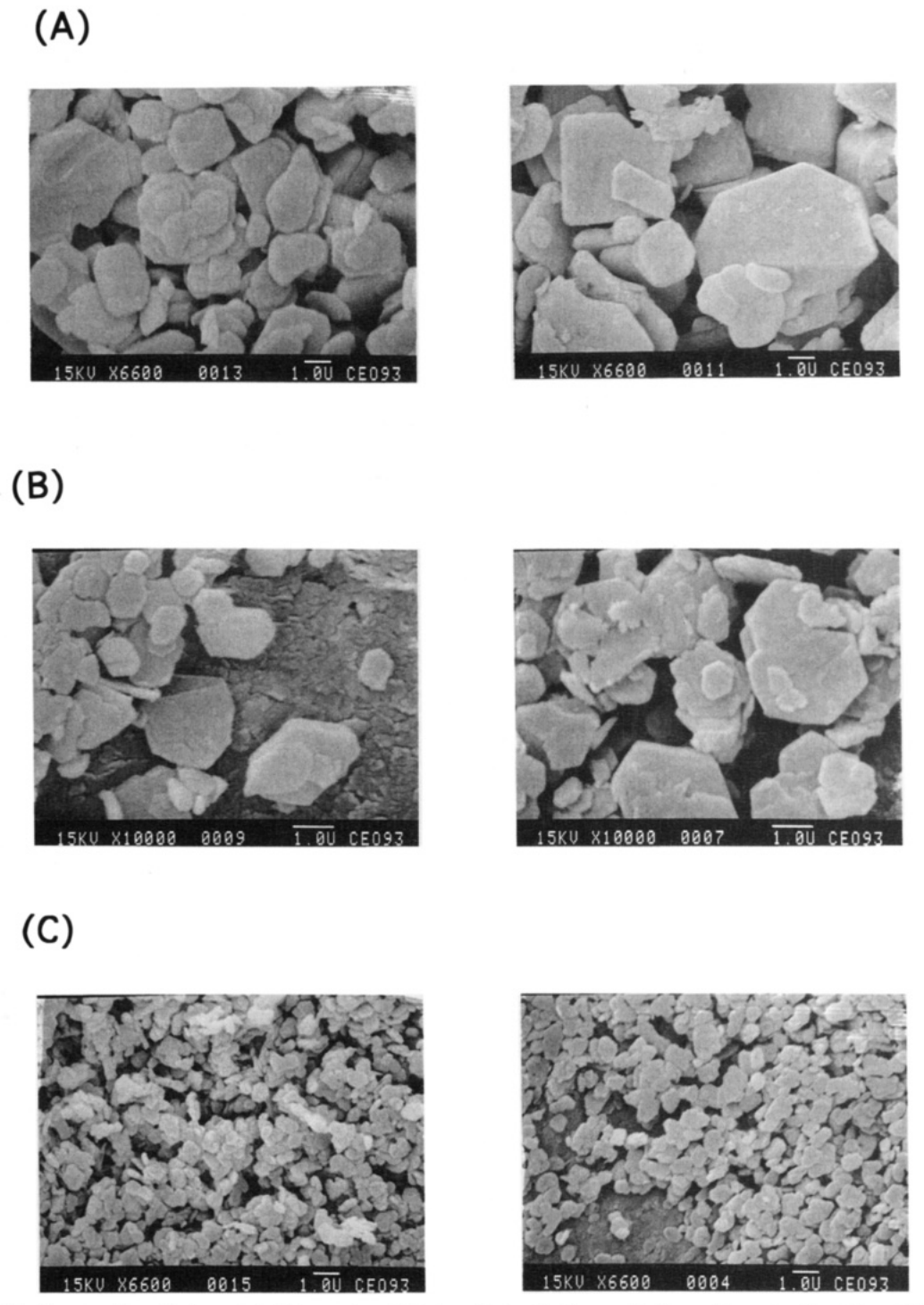

Figure 5. SEM micrographs of intercalated layered metal phosphates before and after polymerization (from left to right): (a) AUP, PUP, (b) A_2ZrP, PZrP, and (c) ATiP, PTiP.

polymerization can be monitored by X-ray diffraction measurements. The X-ray diffraction patterns of AUP as a function of time are shown in Figure 7, where, as the reaction proceeds, the peaks due to AUP gradually disappear and the peaks due to PUP become evident. In contrast to PUP, the interlayer distance dramatically decreases to 20.5 Å for PZrP and 13.25 Å for PTiP. The net expansion of PZrP is ~13.9 Å, suggesting a bilayer of PANI molecules in the interlayer regions, as illustrated in Scheme 1. On the other hand, in PTiP the metal–phosphate layers are only ~6 Å apart which suggests a monolayer of PANI molecules, as illustrated in Scheme 2. In all cases the X-ray diffraction peaks become broader after polymerization due to a decrease in crystallinity. The coherence length along the layer stacking axis decreases from >600 Å in AUP to ~180 Å in PUP, from >400 Å in ATiP to ~180 Å in PTiP and from ~260 Å in A_2ZrP to ~200 Å in PZrP. This is attributed to the increased stacking disorder after polymerization which involves significant movement of monomers and diffusion of oxygen and water in and out of the host crystallites.

Magnetic Properties. The diamagnetic hosts allow the observation of the evolution of the EPR spectroscopic polaron signal of PANI during the polymerization. All precursor compounds are EPR silent. As the reaction proceeds, the compounds start to show symmetric EPR signals which gradually increase in intensity as shown

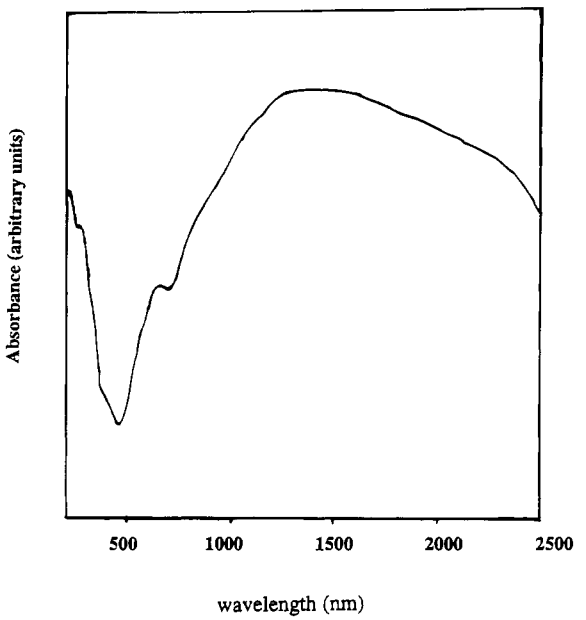

Figure 6. Typical solid state electronic absorption spectrum for PTiP. The strong, very broad absorption in the near-infrared region is attributed to the intercalated PANI molecules which adopt a straight-chain, rodlike, conformation.

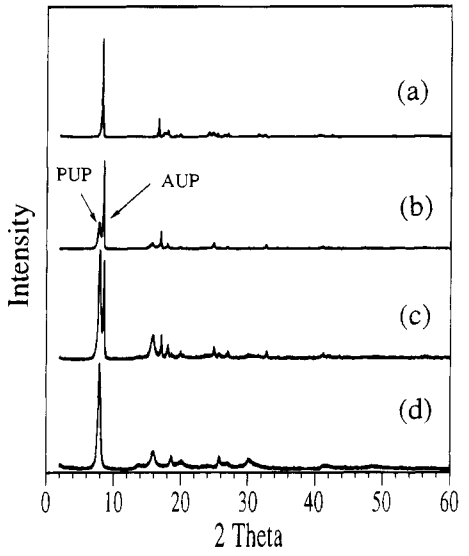

Figure 7. Evolution of powder X-ray diffraction patterns of $(C_6H_5NH_3)_{1.0}UO_2PO_4{\cdot}0.4H_2O$ (AUP) under thermal treatment for (a) 0 week, (b) 1 week, (c) 2 weeks, and (d) 3 weeks.

in Figure 8. The peak widths of these signals decrease with reaction time, indicative of extensive electron delocalization and consistent with polaron formation in PANI. Thus, the peak width (ΔH_{pp}) decreases from 12 to 8 G in PUP, from 7 to 2 G in TiP, and from 15 to 12 G in ZrP. The g values are close to the free electron value of 2.0023. These observations are consistent with the gradual growth of PANI. Bulk PANI in a protonated form was reported with a peak width about <3 G;[25] however, the value can be >10 G with other dopants[26] and also depends on the relative ambient humidity.

The polymerization process can also be monitored with magnetic susceptibility measurements. The appearance of magnetic susceptibility in AUP as a function of reaction time and temperature are shown in Figure 9. When heated, the diamagnetic AUP becomes increasingly paramagnetic. However, the relationship between magnetic susceptibility (χ_m) and temperature does not follow Curie–Weiss law. This is probably due to the presence of Pauli susceptibility which is a property of bulk PANI.[27] Similar behavior was also observed for PTiP and PZrP. The Pauli susceptibility and Curie spin density data (calculated from the susceptibility) are summarized in Table 3. Except for PUP, the amount of Pauli susceptibility for PTiP and PZrP is consistent with reported values for bulk PANI which increase with degree of protonation and lie in the range from 0 to 6.0×10^{-5} emu/mol. The Curie spin density is calculated to be approximately 1 spin/60 rings for PUP and PTiP and 1 spin/135 rings for PZrP. This difference in the case of PZrP is probably because of incomplete polymerization in PZrP where the spin density is diluted by unpolymerized diamagnetic dimers.

Thermogravimetric Analysis Studies. TGA diagrams of PUP, PZrP, and PTiP under O_2 are given in Figure 10. PZrP and PTiP show a single-step weight loss beginning at 400 °C. PUP shows a small weight loss below 100 °C, attributed to water, and two major weight-loss steps at 400 and 600 °C. The weight-loss step starting at 400 °C is attributed to the loss of the intercalated PANI as it thermally breaks up. Compared to bulk PANI (emeraldine salt)[28] (<250 °C), the intercalated PANI molecules show superior thermal stability despite their lower molecular weight. This is due to the spatial confinement and separation of the polymer chains by the metal phosphate layers. The final residues at 900 °C were identified to be $(UO_2)_2(P_2O_7)$, ZrP_2O_7, and TiP_2O_7. Calculated from the TGA data, the stoichiometry is $(PANI)_{2.4}Zr(OPO_3)_2$ for PZrP, $(PANI)_{0.8}Ti(OPO_3)_2$ for PTiP, and $(PANI)_{0.94}UO_2PO_4{\cdot}0.5H_2O$ for PUP, consistent with the elemental analyses. These compositions show that significant amounts of intercalants were lost during polymerization from ATiP and A_2ZrP, and almost none from AUP. The dramatic decrease of interlayer spacing observed for PTiP and PZrP may be in part due to loss of monomer.

Molecular Weight Determination with Gel Permeation Chromatography (GPC). The extracted PANI regardless of inorganic host was partially soluble in NMP. Therefore, the molecular weight of the soluble portions was determined by GPC. The GPC chromatographs of the three extracted PANI residues are shown in Figure 11 where one asymmetric elution band is observed in all cases. The MW of the extracted PANI is summarized in Table 4. All MW values are much lower than that of bulk PANI (prepared chemically or electrochemically) which is in the range of 32 000.[22b,29] It is also evident that the MW of PANI from A_2UP is

(25) (a) Salaneck, W. R.; Liedberg, B.; Inganas, O.; Erlandsson, R.; Lundstrom, I.; MacDiarmid, A. G.; Halpern, M.; Somasiri, N. L. D. *Mol. Cryst. Liq. Cryst.* **1985**, *121*, 191–194. (b) Javadi, H. H. S.; Laversanne, R.; Epstein, A. J.; Kohli, R. K.; Scherr, E. M.; MacDiarmid, A. G. *Synth. Met.* **1989**, *29*, E439–E444.

(26) Cao, Y.; Heeger, A. J. *Synth. Met.* **1990**, *39*, 205–214.

(27) (a) MacDiarmid, A. G.; Chiang, J.-C.; Richter, A. F.; Epstein, A. J. *Synth. Met.* **1987**, *18*, 285–290. (b) Epstein, A. J.; Ginder, J. M.; Zuo, F.; Bigelow, R. W.; Woo, H.-S.; Tanner, D. B.; Richter, A. F.; Huang, W.-S.; MacDiarmid, A. G. *Synth. Met.* **1987**, *18*, 303–309. (c) Geniès, E. M.; Boyle, A.; Lapkowski, M.; Tsintavis, C. *Synth. Met.* **1990**, *36*, 139–182.

(28) Yue, J.; Epstein, A. J.; Zhong, Z.; Gallagher, P. K.; MacDiarmid, A. G. *Synth. Met.* **1991**, *41–43*, 765–768.

(29) (a) Abe, M.; Ohtani, A.; Umemoto, Y.; Akizuki, S.; Ezoe, M.; Higuchi, H.; Nakamoto, K.; Okuno, A.; Noda, Y. *J. Chem. Soc., Chem. Commun.* **1989**, 1736–1738. (b) Geniès, E. M.; Noël, P. *Synth. Met.* **1992**, *46*, 285–292.

Scheme 1

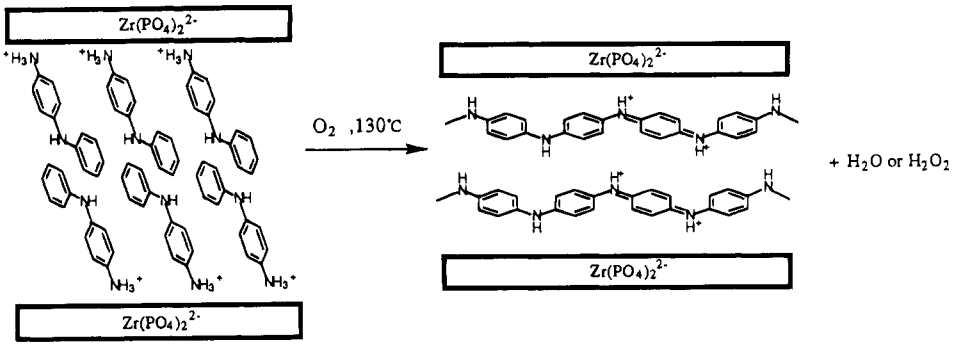

Scheme 2

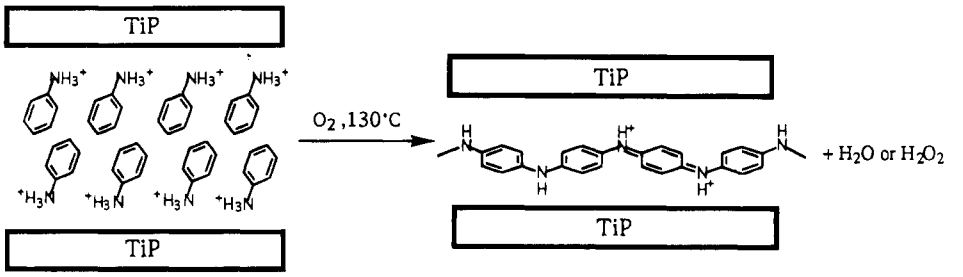

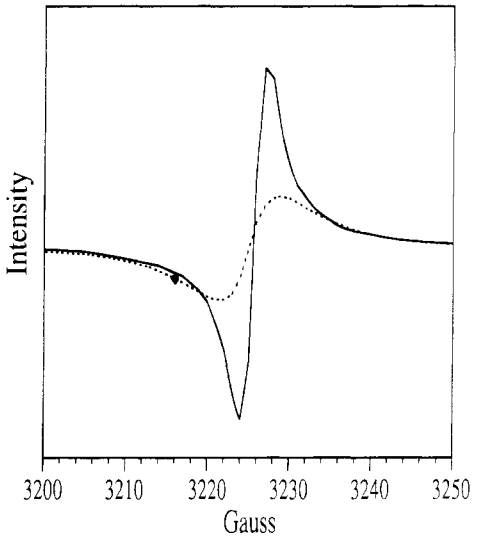

Figure 8. Room-temperature electron paramagnetic resonance spectrum of ATiP after 1 week (- - -) and 3 weeks (—) of thermal treatment.

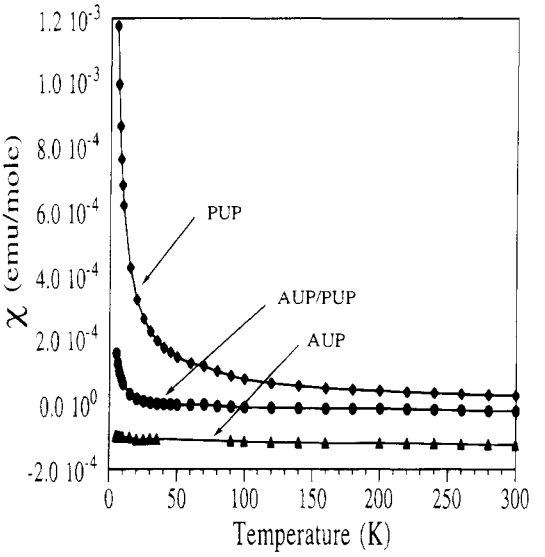

Figure 9. Variable-temperature magnetic susceptibility data of (a) AUP, (b) AUP/PUP mixed phase, and (c) PUP.

higher than that from AUP; however, for the latter the polymer chain distribution length appears more uniform, based on the narrow elution band, see Figure 11. To monitor the progress of polymerization in the intralamellar space of UO_2PO_4, we stopped the reaction at regular intervals, extracted the polymer from the host, and determined its MW by GPC. Surprisingly, we found that the MW of the soluble fraction, after an initial increase in the beginning, decreases with reaction time. For example, polymer isolated from PUP after one week shows a $\bar{M}_w$ of ~14 000 ($\bar{M}_n$ = ~4400). However, polymer isolated after 2 and 3 weeks gives $\bar{M}_w$ of ~7400 ($\bar{M}_n$ = ~4500) and ~4500 ($\bar{M}_n$ = ~2500), respectively. We also observed that the yield of the NMP-soluble fraction decreased with prolonged polymerization time. This result suggests that as the MW increases with time, a certain amount of cross-linking also occurs, as a side reaction, giving rise to an insoluble polymer. Thus, the GPC technique only probes the soluble residue which cannot be further polymerized because of kinetic slow-down. The reason the MW of the soluble fraction is smaller in samples subjected to prolonged heating is probably because it represents kinetically trapped oligomers or short polymer chains in pockets of insoluble high MW polymer.

Table 3. Pauli Susceptibility and Curie Spin Density of PANI/Metal Phosphate Intercalates

compound	Pauli susceptibility (emu/mol)	Curie spin density (ring/spin)
PUP	1.3×10^{-4}	55
PTiP	4.4×10^{-5}	66
PZrP	8.0×10^{-5}	135

Since the conjugated polymers are embedded in the insulating host and cannot be accessed electrically, all PANI intercalated materials described here are bulk insulators. This behavior is similar to that of the

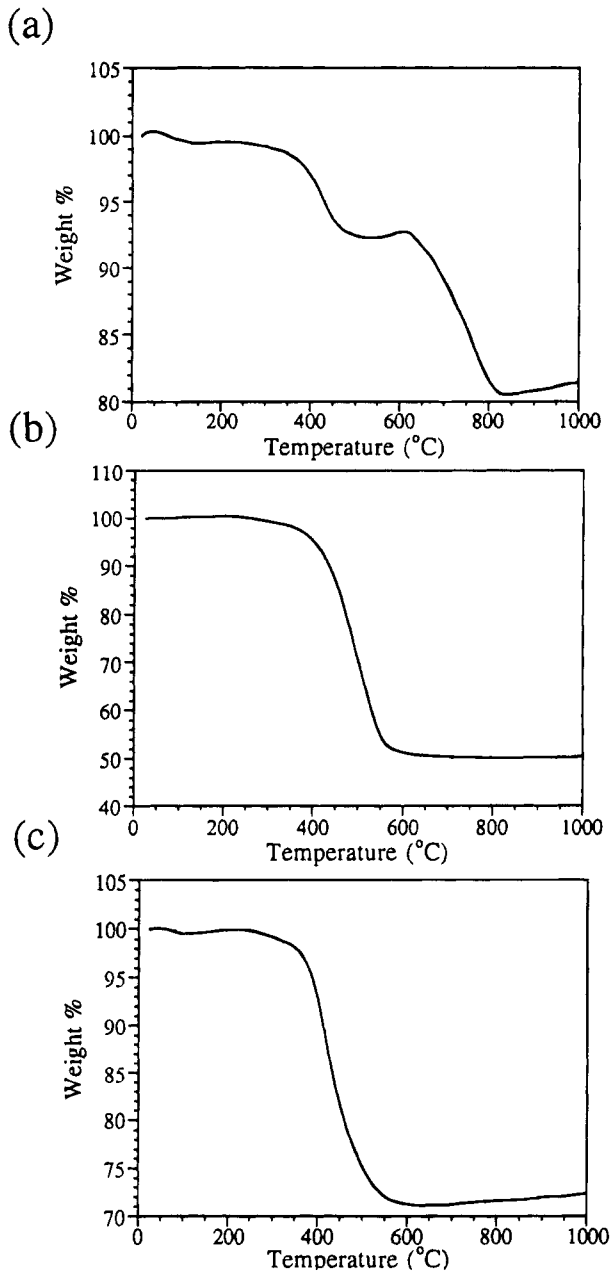

Figure 10. Thermogravimetric analysis diagrams under oxygen for (a) PUP, (b) PZrP, and (c) PTiP.

systems which involve insulators as hosts.[7,8] This, however, does not mean that the organic polymer is not electrically conductive. Isolated from the inorganic hosts the polymer showed room temperature conductivities of 0.01−0.1 S/cm. These values are lower than those of bulk polyaniline and probably reflect the fact that part of the extracted polymer is cross-linked to some extent and part is of lower molecular weight. The

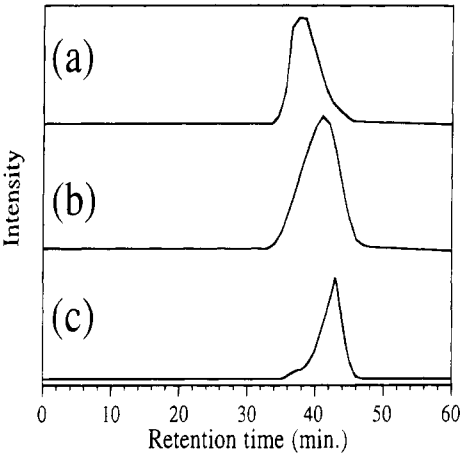

Figure 11. GPC chromatographs of extracted PANI (neutral form) from (a) PUP, (b) PTiP and (c) PZrP. A 0.5 wt % LiCl solution of NMP was used as the eluent.

Table 4. Molecular Weights of Extracted PANI (Soluble Fraction) from Layered Metal Phosphates

	$\bar{M}_n$	$\bar{M}_w$	$\bar{M}_w/\bar{M}_n$
bulk PANI[a]	26000	78000	3.0
PANI extracted from PUP[b]	4400	9200	2.1
PANI extracted from PUP[c]	3000	4500	1.5
PANI extracted from PZrP[d]	2100	2300	1.1
PANI extracted from PTiP	2600	3000	1.2

[a] From ref 22b and reproduced in our laboratory. [b] Precursor was A_2UP. [c] Precursor was AUP. [d] Precursor was A_2ZrP.

conductivity of the polymer chains inside the host may be probed with ac impedance measurements which should give a better picture on the electron delocalization along the conjugated chains.

We have successfully synthesized polyaniline in layered metal phosphates by thermal treatment in ambient oxygen. The spectroscopic and magnetic data of the extracted PANI are comparable with those of bulk PANI prepared chemically, but there is evidence of some cross-linking between molecules in the intralamellar space. The use of PPDA as a monomer for PANI did not yield shorter reaction times, but in the cases of uranyl phosphate it gave longer polymer chains. The results reported here indicate that oxygen may be a convenient and clean reagent for topotactic oxidative polymerization of monomers occluded in inorganic galleries. Perhaps lower polymerization temperatures could be achieved with ozone.

Acknowledgment. Financial Support from the National Science Foundation (DMR-93-06385) is gratefully acknowledged. This work made use of the SEM facilities of the Center for Electron Optics at Michigan State University.

CM950068R